Research Article | Vol. 9, No. 9 | 1 Sep 2018 | BIOMEDICAL OPTICS EXPRESS 4196
Biomedical Optics EXPRESS

Feasibility of using optical coherence tomography to detect radiation-induced fibrosis and residual cancer extent after neoadjuvant chemo-radiation therapy: an ex vivo study

POUYA JELVEHGARAN,[1,2,3,*] TANJA ALDERLIESTEN,[2] GIOTA GEORGIOU,[2] SYBREN L. MEIJER,[4] PAUL R. BLOEMEN,[1] LIUDMILA L. KODACH,[4] HANNEKE W. M. VAN LAARHOVEN,[5] MARK I. VAN BERGE HENEGOUWEN,[6] MAARTEN C. C. M. HULSHOF,[2] COEN R. N. RASCH,[2] TON G. VAN LEEUWEN,[1] JOHANNES F. DE BOER,[3] MARTIJN DE BRUIN,[1,7] AND MARCEL VAN HERK[1,8]

[1]*Department of Biomedical Engineering and Physics, Amsterdam UMC, University of Amsterdam, Amsterdam 1105 AZ, The Netherlands*
[2]*Department of Radiation Oncology, Amsterdam UMC, University of Amsterdam, Amsterdam 1105 AZ, The Netherlands*
[3]*Institute for Laser Life and Biophotonics Amsterdam, Department of Physics and Astronomy, VU University Amsterdam, Amsterdam 1081 HV, The Netherlands*
[4]*Department of Pathology, Amsterdam UMC, University of Amsterdam, Amsterdam 1105 AZ, The Netherlands*
[5]*Department of Medical Oncology, Amsterdam UMC and Cancer Center Amsterdam, University of Amsterdam, Amsterdam 1105 AZ, The Netherlands*
[6]*Department of Surgery, Amsterdam UMC and Cancer Center Amsterdam, University of Amsterdam, Amsterdam 1105 AZ, The Netherlands*
[7]*Department of Urology, Amsterdam UMC, University of Amsterdam, Amsterdam 1105 AZ, The Netherlands*
[8]*Manchester Cancer Research Centre, Division of Cancer Science, School of Medical Sciences, Faculty of Biology, Medicine and Health, University of Manchester, Manchester Academic Health Sciences Centre, Manchester M13 9PL, UK*
**p.jelvehgaran@amc.uva.nl*

Abstract: Treatment of resectable esophageal cancer includes neoadjuvant chemo-radiation therapy (nCRT) followed by esophagectomy in operable patients. High-risk surgery may have been avoided in patients with a pathological complete response (pCR). We investigated the feasibility of optical coherence tomography (OCT) to detect residual cancer and radiation-induced fibrosis in 10 esophageal cancer patients that underwent nCRT followed by esophagectomy. We compared our OCT findings with histopathology. Overall, OCT was able to differentiate between healthy tissue, fibrotic tissue, and residual cancer with a sensitivity and specificity of 79% and 67%, respectively. Hence, OCT has the potential to add to the assessment of a pCR.

OCIS codes: (170.0170) Medical optics and biotechnology; (170.1610) Clinical applications; (170.2150) Endoscopic imaging.

References and links

1. F. Roeder, N. H. Nicolay, T. Nguyen, L. Saleh-Ebrahimi, V. Askoxylakis, T. Bostel, F. Zwicker, J. Debus, C. Timke, and P. E. Huber, "Intensity modulated radiotherapy (IMRT) with concurrent chemotherapy as definitive treatment of locally advanced esophageal cancer," Radiat. Oncol. **9**(9), 191 (2014).
2. A. Pennathur and J. D. Luketich, "Resection for esophageal cancer: strategies for optimal management," Ann. Thorac. Surg. **85**(2), S751–S756 (2008).

#330772 https://doi.org/10.1364/BOE.9.004196
Journal © 2018 Received 3 May 2018; revised 3 Jul 2018; accepted 2 Aug 2018; published 14 Aug 2018

Biomedical Optics EXPRESS

3. M. Stahl, M. Stuschke, N. Lehmann, H.-J. Meyer, M. K. Walz, S. Seeber, B. Klump, W. Budach, R. Teichmann, M. Schmitt, G. Schmitt, C. Franke, and H. Wilke, "Chemoradiation with and without surgery in patients with locally advanced squamous cell carcinoma of the esophagus," J. Clin. Oncol. **23**(10), 2310–2317 (2005).
4. J. D. Urschel and H. Vasan, "A meta-analysis of randomized controlled trials that compared neoadjuvant chemoradiation and surgery to surgery alone for resectable esophageal cancer," Am. J. Surg. **185**(6), 538–543 (2003).
5. F. Fiorica, D. Di Bona, F. Schepis, A. Licata, L. Shahied, A. Venturi, A. M. Falchi, A. Craxì, and C. Cammà, "Preoperative chemoradiotherapy for oesophageal cancer: a systematic review and meta-analysis," Gut **53**(7), 925–930 (2004).
6. P. van Hagen, M. C. C. M. Hulshof, J. J. B. van Lanschot, E. W. Steyerberg, M. I. van Berge Henegouwen, B. P. Wijnhoven, D. J. Richel, G. A. Nieuwenhuijzen, G. A. Hospers, J. J. Bonenkamp, M. A. Cuesta, R. J. Blaisse, O. R. Busch, F. J. ten Kate, G. J. Creemers, C. J. Punt, J. T. Plukker, H. M. Verheul, E. J. Spillenaar Bilgen, H. van Dekken, M. J. van der Sangen, T. Rozema, K. Biermann, J. C. Beukema, A. H. Piet, C. M. van Rij, J. G. Reinders, H. W. Tilanus, A. van der Gaast, and A. Van Der Gaast, "Preoperative Chemoradiotherapy for Esophageal or Junctional Cancer," N. Engl. J. Med. **366**(22), 2074–2084 (2012).
7. J. Shapiro, J. J. B. van Lanschot, M. C. C. M. Hulshof, P. van Hagen, M. I. van Berge Henegouwen, B. P. L. Wijnhoven, H. W. M. van Laarhoven, G. A. P. Nieuwenhuijzen, G. A. P. Hospers, J. J. Bonenkamp, M. A. Cuesta, R. J. B. Blaisse, O. R. C. Busch, F. J. W. Ten Kate, G. M. Creemers, C. J. A. Punt, J. T. M. Plukker, H. M. W. Verheul, E. J. S. Bilgen, H. van Dekken, M. J. C. van der Sangen, T. Rozema, K. Biermann, J. C. Beukema, A. H. M. Piet, C. M. van Rij, J. G. Reinders, H. W. Tilanus, E. W. Steyerberg, and A. van der Gaast, "Neoadjuvant chemoradiotherapy plus surgery versus surgery alone for oesophageal or junctional cancer (CROSS): long-term results of a randomised controlled trial," Lancet Oncol. **16**(9), 1090–1098 (2015).
8. M. C. J. Anderegg, E. J. de Groof, S. S. Gisbertz, R. J. Bennink, S. M. Lagarde, J. H. G. Klinkenbijl, M. G. W. Dijkgraaf, J. J. G. H. M. Bergman, M. C. C. M. Hulshof, H. W. M. van Laarhoven, and M. I. van Berge Henegouwen, "18F-FDG PET-CT after neoadjuvant chemoradiotherapy in esophageal cancer patients to optimize surgical decision making," PLoS One **10**(11), e0133690 (2015).
9. J. D. Birkmeyer, A. E. Siewers, E. V. Finlayson, T. A. Stukel, F. L. Lucas, I. Batista, H. G. Welch, and D. E. Wennberg, "Hospital volume and surgical mortality in the United States," N. Engl. J. Med. **346**(15), 1128–1137 (2002).
10. A. M. Brown, M. J. Pucci, A. C. Berger, T. Tatarian, N. R. Evans, I. I. I. Ernest, and L. R. Francesco, "A standardized comparison of peri-operative complications after minimally invasive esophagectomy : Ivor Lewis versus McKeown," Surg. Endosc. **32**, 204–211 (2017).
11. D. Pfirrmann, S. Tug, O. Brosteanu, M. Mehdorn, M. Busse, P. P. Grimminger, F. Lordick, T. Glatz, J. Hoeppner, H. Lang, P. Simon, and I. Gockel, "Internet-based perioperative exercise program in patients with Barrett ' s carcinoma scheduled for esophagectomy [iPEP - study] a prospective randomized- controlled trial," BMC Cancer **17**, 413 (2017).
12. J. Guo, C. Q. Li, M. Li, X. L. Zuo, T. Yu, J. W. Liu, J. Liu, G. J. Kou, and Y. Q. Li, "Diagnostic value of probe-based confocal laser endomicroscopy and high-definition virtual chromoendoscopy in early esophageal squamous neoplasia," Gastrointest. Endosc. **81**(6), 1346–1354 (2015).
13. A. M. Monjazeb, G. Riedlinger, M. Aklilu, K. R. Geisinger, G. Mishra, S. Isom, P. Clark, E. A. Levine, and A. W. Blackstock, "Outcomes of patients with esophageal cancer staged with [^{18}F]fluorodeoxyglucose positron emission tomography (FDG-PET): can postchemoradiotherapy FDG-PET predict the utility of resection?" J. Clin. Oncol. **28**(31), 4714–4721 (2010).
14. L. Bedenne, P. Michel, O. Bouché, C. Milan, C. Mariette, T. Conroy, D. Pezet, B. Roullet, J. F. Seitz, J. P. Herr, B. Paillot, P. Arveux, F. Bonnetain, and C. Binquet, "Chemoradiation followed by surgery compared with chemoradiation alone in squamous cancer of the esophagus: FFCD 9102," J. Clin. Oncol. **25**(10), 1160–1168 (2007).
15. J.-F. Bosset, M. Gignoux, J.-P. Triboulet, E. Tiret, G. Mantion, D. Elias, P. Lozach, J.-C. Ollier, J. J. Pavy, M. Mercier, T. Sahmoud, and M. B. Tarek, "Chemoradiotherapy followed by surgery compared with surgery alone in squamous-cell cancer of the esophagus," N. Engl. J. Med. **337**(3), 161–167 (1997).
16. P. Pimentel-Nunes, M. Dinis-Ribeiro, T. Ponchon, A. Repici, M. Vieth, A. De Ceglie, A. Amato, F. Berr, P. Bhandari, A. Bialek, M. Conio, J. Haringsma, C. Langner, S. Meisner, H. Messmann, M. Morino, H. Neuhaus, H. Piessevaux, M. Rugge, B. P. Saunders, M. Robaszkiewicz, S. Seewald, S. Kashin, J. M. Dumonceau, C. Hassan, and P. H. Deprez, "Endoscopic submucosal dissection: European Society of Gastrointestinal Endoscopy (ESGE) Guideline," Endoscopy **47**(9), 829–854 (2015).
17. B. J. Noordman, J. Shapiro, M. C. Spaander, K. K. Krishnadath, H. W. van Laarhoven, M. I. van Berge Henegouwen, G. A. Nieuwenhuijzen, R. van Hillegersberg, M. N. Sosef, E. W. Steyerberg, B. P. Wijnhoven, and J. J. B. van Lanschot, "Accuracy of detecting residual disease after cross neoadjuvant chemoradiotherapy for esophageal cancer (preSANO Trial): rationale and protocol," JMIR Res. Protoc. **4**(2), e79 (2015).
18. A. J. E. Seely, J. Ivanovic, J. Threader, A. Al-Hussaini, D. Al-Shehab, T. Ramsay, S. Gilbert, D. E. Maziak, F. M. Shamji, and R. S. Sundaresan, "Systematic classification of morbidity and mortality after thoracic surgery," Ann. Thorac. Surg. **90**(3), 936–942, discussion 942 (2010).
19. S. H. Bailey, D. A. Bull, D. H. Harpole, J. J. Rentz, L. A. Neumayer, T. N. Pappas, J. Daley, W. G. Henderson, B. Krasnicka, S. F. Khuri, and D. E. Wood, "Outcomes after esophagectomy: A ten-year prospective cohort," Ann. Thorac. Surg. **75**(1), 217–222 (2003).

Biomedical Optics EXPRESS

20. C. L. Donohoe, E. McGillycuddy, and J. V. Reynolds, "Long-term health-related quality of life for disease-free esophageal cancer patients," World J. Surg. **35**(8), 1853–1860 (2011).
21. R. L. G. M. Blom, W. M. J. Schreurs, H. J. Belgers, L. E. Oostenbrug, R. F. A. Vliegen, and M. N. Sosef, "The value of post-neoadjuvant therapy PET-CT in the detection of interval metastases in esophageal carcinoma," Eur. J. Surg. Oncol. **37**(9), 774–778 (2011).
22. H. M. Salahudeen, A. Balan, K. Naik, S. Mirsadraee, and A. F. Scarsbrook, "Impact of the introduction of integrated PET-CT into the preoperative staging pathway of patients with potentially operable oesophageal carcinoma," Clin. Radiol. **63**(7), 765–773 (2008).
23. K. Thurau, D. Palmes, C. Franzius, E. Minin, N. Senninger, K. U. Juergens, and M. Bruewer, "Impact of PET-CT on primary staging and response control on multimodal treatment of esophageal cancer," World J. Surg. **35**(3), 608–616 (2011).
24. R. Wong, C. Walker-Dilks, and A. Raifu, "Evidence-based guideline recommendations on the use of positron emission tomography imaging in oesophageal cancer," Clin. Oncol. **24**(2), 86–104 (2012).
25. H. L. van Westreenen, M. Westerterp, G. W. Sloof, H. Groen, P. M. M. Bossuyt, P. L. Jager, E. F. Comans, H. M. van Dullemen, P. Fockens, J. Stoker, E. J. van der Jagt, J. J. B. van Lanschot, and J. T. M. Plukker, "Limited additional value of positron emission tomography in staging oesophageal cancer," Br. J. Surg. **94**(12), 1515–1520 (2007).
26. R. Langer and K. Becker, "Tumor regression grading of gastrointestinal cancers after neoadjuvant therapy," Virchows Arch. **472**(2), 175–186 (2018).
27. A.-M. Mandard, F. Dalibard, J.-C. Mandard, J. Marnay, M. Henry-Amar, J.-F. Petiot, A. Roussel, J.-H. Jacob, P. Segol, G. Samama, J.-M. Ollivier, S. Bonvalot, and M. Gignoux, "Pathologic assessment of tumor regression after preoperative chemoradiotherapy of esophageal carcinoma: clinicopathologic correlations," Cancer **73**(11), 2680–2686 (1994).
28. P. Jelvehgaran, T. Alderliesten, J. J. A. Weda, M. de Bruin, D. J. Faber, M. C. C. M. Hulshof, T. G. van Leeuwen, M. van Herk, and J. F. de Boer, "Visibility of fiducial markers used for image-guided radiation therapy on optical coherence tomography for registration with CT: an esophageal phantom study," Med. Phys. **44**(12), 6570–6582 (2017).
29. D. Huang, E. Swanson, C. Lin, J. Schuman, W. Stinson, W. Chang, M. Hee, T. Flotte, K. Gregory, C. Puliafito, and A. Et, "Optical coherence tomography," Science **254**, 1178–1181 (1991).
30. S. H. Yun, G. J. Tearney, B. J. Vakoc, M. Shishkov, W. Y. Oh, A. E. Desjardins, M. J. Suter, R. C. Chan, J. A. Evans, I.-K. Jang, N. S. Nishioka, J. F. de Boer, and B. E. Bouma, "Comprehensive volumetric optical microscopy in vivo," Nat. Med. **12**(12), 1429–1433 (2006).
31. H. C. Wolfsen, P. Sharma, M. B. Wallace, C. Leggett, G. Tearney, and K. K. Wang, "Safety and feasibility of volumetric laser endomicroscopy in patients with Barrett's esophagus (with videos)," Gastrointest. Endosc. **82**(4), 631–640 (2015).
32. A. Swager, D. F. Boerwinkel, D. M. de Bruin, B. L. Weusten, D. J. Faber, S. L. Meijer, T. G. van Leeuwen, W. L. Curvers, and J. J. Bergman, "Volumetric laser endomicroscopy in Barrett's esophagus: a feasibility study on histological correlation," Dis. Esophagus **29**(6), 505–512 (2016).
33. M. J. Suter, M. J. Gora, G. Y. Lauwers, T. Arnason, J. Sauk, K. A. Gallagher, L. Kava, K. M. Tan, A. R. Soomro, T. P. Gallagher, J. A. Gardecki, B. E. Bouma, M. Rosenberg, N. S. Nishioka, and G. J. Tearney, "Esophageal-guided biopsy with volumetric laser endomicroscopy and laser cautery marking: a pilot clinical study," Gastrointest. Endosc. **79**(6), 886–896 (2014).
34. C. Sun, F. Nolte, K. H. Y. Cheng, B. Vuong, K. K. C. Lee, B. A. Standish, B. Courtney, T. R. Marotta, A. Mariampillai, and V. X. D. Yang, "In vivo feasibility of endovascular Doppler optical coherence tomography," Biomed. Opt. Express **3**(10), 2600–2610 (2012).
35. M. T. J. Bus, B. G. Muller, D. M. de Bruin, D. J. Faber, G. M. Kamphuis, T. G. van Leeuwen, T. M. de Reijke, and J. J. M. C. H. de la Rosette, "Volumetric in Vivo Visualization of Upper Urinary Tract Tumors Using Optical Coherence Tomography: A Pilot Study," J. Urol. **190**(6), 2236–2242 (2013).
36. P. Cernohorsky, D. M. de Bruin, M. van Herk, J. Bras, D. J. Faber, S. D. Strackee, and T. G. van Leeuwen, "In-situ imaging of articular cartilage of the first carpometacarpal joint using co-registered optical coherence tomography and computed tomography," J. Biomed. Opt. **17**(6), 060501 (2012).
37. G. J. Tearney, M. E. Brezinski, B. E. Bouma, S. A. Boppart, C. Pitris, J. F. Southern, and J. G. Fujimoto, "In vivo endoscopic optical biopsy with optical coherence tomography," Science **276**(5321), 2037–2039 (1997).
38. A. Sergeev, V. Gelikonov, G. Gelikonov, F. Feldchtein, R. Kuranov, N. Gladkova, N. Shakhova, L. Snopova, A. Shakhov, I. Kuznetzova, A. Denisenko, V. Pochinko, Y. Chumakov, and O. Streltzova, "In vivo endoscopic OCT imaging of precancer and cancer states of human mucosa," Opt. Express **1**(13), 432–440 (1997).
39. B. E. Bouma, G. J. Tearney, C. C. Compton, and N. S. Nishioka, "High-resolution imaging of the human esophagus and stomach in vivo using optical coherence tomography," Gastrointest. Endosc. **51**(4), 467–474 (2000).
40. P. Jelvehgaran, D. M. de Bruin, F. J. Salguero, G. R. Borst, J.-Y. Song, T. G. van Leeuwen, J. F. de Boer, T. Alderliesten, and M. van Herk, "Feasibility of using optical coherence tomography to detect acute radiation-induced esophageal damage in small animal models," J. Biomed. Opt. **23**(4), 1–12 (2018).
41. K. Kobayashi, J. A. Izatt, M. D. Kulkarni, J. Willis, and M. V. Sivak, Jr., "High-resolution cross-sectional imaging of the gastrointestinal tract using optical coherence tomography: preliminary results," Gastrointest. Endosc. **47**(6), 515–523 (1998).

Biomedical Optics EXPRESS

42. Y. Chen, A. D. Aguirre, P.-L. Hsiung, S.-W. Huang, H. Mashimo, J. M. Schmitt, and J. G. Fujimoto, "Effects of axial resolution improvement on optical coherence tomography (OCT) imaging of gastrointestinal tissues," Opt. Express **16**(4), 2469–2485 (2008).
43. J. A. Evans, J. M. Poneros, B. E. Bouma, J. Bressner, E. F. Halpern, M. Shishkov, G. Y. Lauwers, M. M. Kenudson, N. S. Nishioka, and G. J. Tearney, "Optical coherence tomography to identify intramucosal carcinoma and high-grade dysplasia in Barrett's esophagus," Clin. Gastroenterol. Hepatol. **4**(1), 38–43 (2006).
44. J. W. Wolthaus, M. van Herk, S. H. Muller, J. S. Belderbos, J. V. Lebesque, J. A. de Bois, M. M. Rossi, and E. M. Damen, "Fusion of respiration-correlated PET and CT scans: correlated lung tumour motion in anatomical and functional scans," Phys. Med. Biol. **50**(7), 1569–1583 (2005).
45. A. Sergeev, V. Gelikonov, G. Gelikonov, F. Feldchtein, R. Kuranov, N. Gladkova, N. Shakhova, L. Snopova, A. Shakhov, I. Kuznetzova, A. Denisenko, V. Pochinko, Y. Chumakov, and O. Streltzova, "In vivo endoscopic OCT imaging of precancer and cancer states of human mucosa," Opt. Express **1**(13), 432–440 (1997).
46. K. F. Siu, H. C. Cheung, and J. Wong, "Shrinkage of the esophagus after resection for carcinoma," Ann. Surg. **203**(2), 173–176 (1986).
47. E. P. M. van Vliet, M. J. C. Eijkemans, J. W. Poley, E. W. Steyerberg, E. J. Kuipers, and P. D. Siersema, "Staging of esophageal carcinoma in a low-volume EUS center compared with reported results from high-volume centers," Gastrointest. Endosc. **63**(7), 938–947 (2006).
48. W. Hatta, K. Uno, T. Koike, K. Iijima, N. Asano, A. Imatani, and T. Shimosegawa, "A prospective comparative study of optical coherence tomography and EUS for tumor staging of superficial esophageal squamous cell carcinoma," Gastrointest. Endosc. **76**(3), 548–555 (2012).
49. A. Das, M. V. Sivak, Jr., A. Chak, R. C. Wong, V. Westphal, A. M. Rollins, J. Willis, G. Isenberg, and J. A. Izatt, "High-resolution endoscopic imaging of the GI tract: a comparative study of optical coherence tomography versus high-frequency catheter probe EUS," Gastrointest. Endosc. **54**(2), 219–224 (2001).
50. W. Hatta, K. Uno, T. Koike, S. Yokosawa, K. Iijima, A. Imatani, and T. Shimosegawa, "Optical coherence tomography for the staging of tumor infiltration in superficial esophageal squamous cell carcinoma," Gastrointest. Endosc. **71**(6), 899–906 (2010).

1. Introduction

Surgical esophageal resection or esophagectomy is the treatment of choice for patients with resectable esophageal cancer (>T2) after neoadjuvant chemo-radiation therapy (nCRT) [1,2]. Addition of nCRT to surgery showed survival benefit for operable patients [3–7]. Esophagectomy is a complicated procedure with substantial morbidity and mortality [8–12]. The 30-day postoperative mortality rate that exceeds 2% [3,13–16]. Further, esophagectomy negatively affects long term quality of life [17–20].

In patients with a complete response to nCRT an organ sparing approach could be followed, possibly resulting in a better quality of life [17]. Therefore, it is crucial to differentiate patients with pathological complete response (pCR) from pathological non-complete responders after nCRT [8,21]. The standard clinical evaluation of the nCRT effect is endoscopy with random mucosal biopsy, but standard biopsies are not accurate enough to detect a true pCR [17]. Using [^{18}F] fluorodeoxyglucose positron emission tomography (FDG-PET) in combination with computed tomography (CT) — for anatomical reference — has been proven to detect metastasis and assess local treatment response [8,22–24]. However, numerous false-positive and false-negative results have been reported for FDG-PET partly due to its low resolution [25]. If we could more precisely identify patients with a pCR to nCRT beyond FDG-PET knowledge, we may prevent unnecessary surgery. Histopathology analysis of resected specimens after nCRT shows radiation-induced fibrosis and residual cancer with other injuries such as inflammation and resorptive changes with infiltrates of foamy histiocytes (Fig. 1) [26]. Tumor regression grading (TRG) systems exist to report the amount of regressive changes based on the relation between the amount of radiation-induced fibrosis in contrast with residual tumor/cancer [26,27]. During radiation therapy (RT) planning on CT, a margin is added around the gross tumor volume (GTV) to include subclinical disease spread to create the clinical target volume (CTV) [28]. A further margin is added to the CTV to account for treatment uncertainties — obtaining the planning target volume (PTV) [1,28]. Radiation-induced fibrosis is expected to be present in the whole PTV while residual cancer is expected to correspond mostly with the GTV area.

Optical coherence tomography (OCT) is a minimally invasive cross-sectional imaging technique to acquire high resolution (10 μm) 3D images based on the backscattering of light.

Biomedical Optics EXPRESS

The depth of penetration is limited to 2–3 mm [29,30]. OCT imaging systems equipped with inflatable cylindrical catheters using single rotating fibers facilitate in vivo endoscopic OCT imaging of the esophagus [31–38]. Studies demonstrated the capability of OCT to identify esophageal wall layers from epithelium to muscular propria and glandular structure on a microscopic level [39–43]. Hence, we hypothesize that OCT can potentially differentiate between residual cancer, radiation-induced fibrosis, and normal esophageal tissue.

In this study, we investigated the feasibility of using OCT to detect radiation-induced fibrosis and esophageal residual cancer in 10 patients treated with nCRT, using ex-vivo imaging of fresh specimens after esophagectomy. We matched our findings with histopathology as the gold standard. Identical with histopathology, our pCR criterium is to not observe any residual cancer in OCT images. In vivo OCT will show increased resolution due to lack of shrinkage. Therefore, we compared the length of the PTV with the length of the post nCRT radiation-induced fibrosis region in histopathology and the length of the GTV with the length of the residual cancer in histopathology. Comparing GTV and histopathology provides additional information regarding uncertainties in the GTV definition, which OCT may enhance.

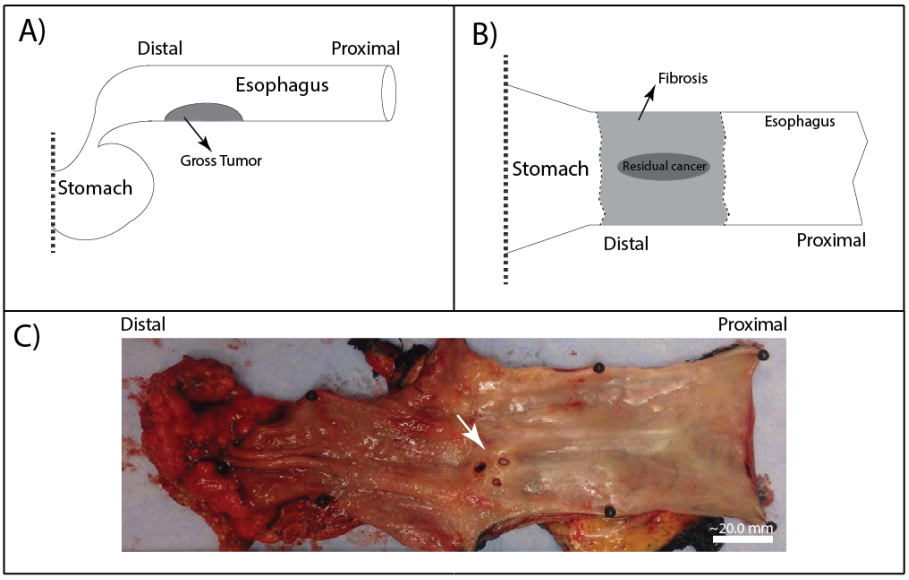

Fig. 1. A) The schematic demonstrates a gross tumor inside an intact esophagus prior to nCRT treatment. B) The schematic shows residual cancer and radiation-induced fibrosis as results of nCRT treatment in a cut open esophageal specimen after esophagectomy. C) The figure shows a resected esophageal specimen from patient 7 pinned to a styrene foam board. The white arrow points to the location of the primary tumor area.

2. Methods

From 10 patients with potentially curative esophageal cancer with suspected residual disease, resected specimens were collected, scanned with OCT on a dedicated scanning apparatus, and the histopathology analyzed. We compared OCT and histopathology results guided by histopathology as the gold standard.

2.1 Patient selection

We acquired ex vivo OCT images from esophageal excision specimens of 10 operable nCRT treated patients (mean age 63.2 years [SD = 8.8], 7 male, 3 female) who consecutively underwent esophagectomy from October 2016 to December 2016 (Table 1, Fig. 1). We solely included patients with positive FDG-PET imaging for residual cancer prior to surgery, based

Biomedical Optics EXPRESS

on the radiology report. The FDG-PET/CT imaging was performed about two weeks prior to surgery.

2.2 General specimen preparation

Freshly resected esophageal specimens were cut open longitudinally and pinned to styrene foam boards (for optimal fixation), according to the standard tissue fixation protocol (Fig. 1). The histopathology method of pinning the specimen to a styrene foam board kept shrinkage at a minimal level. For the first 5 patients, OCT was made of the fresh specimen prior to the pinning step, for the remainder of the patients the OCT imaging was acquired after the pinning step. Next, the esophageal specimens were laterally inked using two colors for orientation reference. We localized the primary tumor region through palpation, visually, and by taking into account the pre-operative reports regarding the primary position of the gross tumor.

2.3 Specimen preparation for OCT

Fiducial markers were used to co-localize the OCT and histopathology findings. In addition, the markers were used to estimate shrinkage of the esophageal specimen after formalin fixation. We solely considered longitudinal shrinkage, since the longitudinal tumor extent has the greatest uncertainty.

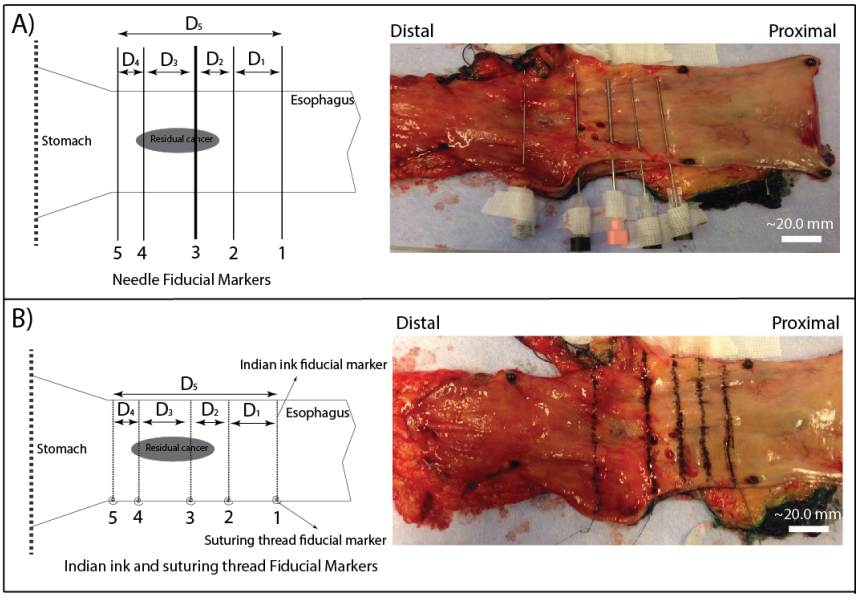

Fig. 2. A) This schematic diagram and image show the needle fiducial markers inserted prior to OCT imaging (patient 7). The third fiducial marker was larger in diameter for better identification on OCT. B) The schematic diagram and image demonstrate the Indian ink and suturing thread markings made after OCT imaging and prior to tissue fixation.

We applied three materials as fiducial markers: 1. hollow injection needles (normal spinal needle, BD Medical Systems); 2. Indian ink (Royal Talent, Apeldoorn, the Netherlands); 3. suturing threads (normal surgical needle with thread), 0.5 mm diameter. We inserted four 18.0-gauge needles and one 22.0-gauge needle into the esophageal specimen, which were well visible on the OCT. Because of safety concerns during tissue preparation, we replaced the needles with ink markings prior to the fixation and cutting of the specimen. For this purpose, the tissue was perforated with small drops of ink alongside the needle trajectory using a 22.0-gauge needle. Because formalin fixation could diminish the color, we also used

Biomedical Optics EXPRESS

suturing threads to label the beginning of each inked marked trajectory to guide the pathologists (Fig. 2).

Two fiducial markers were placed at the proximal esophageal OCT region of interest (ROI). Two fiducial markers were placed at the proximal and distal borders of the residual cancer burden area – and one in the distal part of the specimen — close to the stomach level. The reference marker was the one at the distal border of the primary tumor region. We measured the distance between the markers several times to estimate tissue shrinkage and as validation of the distances found in OCT imaging. After marker placement, we acquired photos from (the pinned) specimen using a digital camera to determine the ROI for the OCT imaging.

2.4 OCT imaging

We used a commercial Santec Inner Vision 2000 swept-source OCT imaging system (Santec Corporation, Komaki, Aichi, Japan). The OCT imaging system produces images with axial resolution of 18.0 µm and lateral resolution of 25.0 µm using light at a central wavelength of 1310.0 nm and sweep rate of 50.0 kHz. The OCT system comes with a hand-held probe that scans volumes of 20.0 X 20.0 X 8.8 mm^3 in 3D, taking about 20.0 seconds per scan. Dispersion compensation was performed to compensate for the dispersive elements — 6.0 mm thick glass in the imaging path — using the reflection of the glass surface. In order to scan the whole area of interest of a human esophagus, multiple scans must be combined. A dedicated scanning apparatus was used that consists of a moving stage that precisely relocates the hand-held probe in sagittal, coronal, and axial planes, maintaining a uniform angle and level (Fig. 3). The specimen is spread out, innermost mucosa layer touching a 180.0 x 360.0 mm^2 gridded glass plate (6.0 mm thick), held in place by a water-filled balloon placed on either the specimen or the styrene foam board. Tape was attached to the heads and tails of the fiducial markers. This would prevent the needle fiducial markers from moving, which may result in changes in distance measurements. The handheld OCT probe scans the esophageal specimen from underneath the glass plate (Fig. 3). We tilted the hand-held OCT probe to avoid artifacts due to reflection from the glass. Accurate movement and relocation of the probe allows a consistent overlap between the acquired scans, which is crucial for merging the data into a single esophageal scan. A scan overlap of 2 mm was created by translating the stage 18.0 mm between acquisitions (Fig. 4).

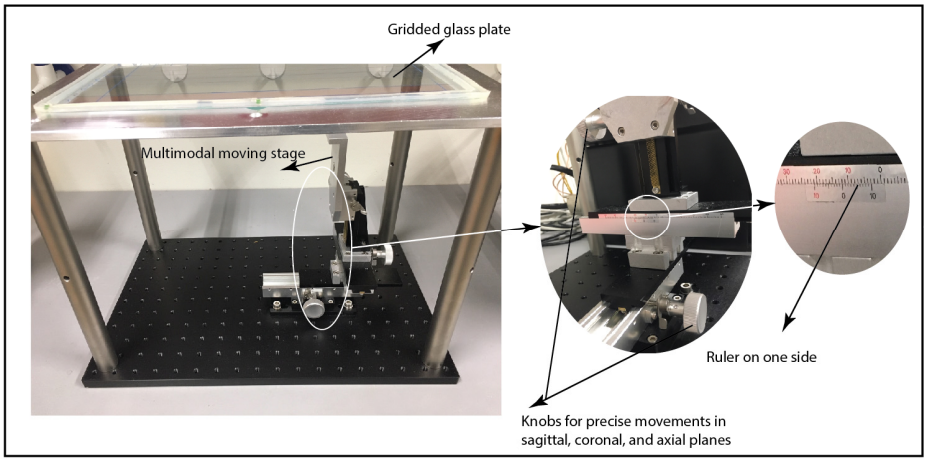

Fig. 3. Our dedicated scanning setup with moving stage to precisely position the hand-held probe in sagittal, coronal, and axial planes.

Biomedical Optics EXPRESS

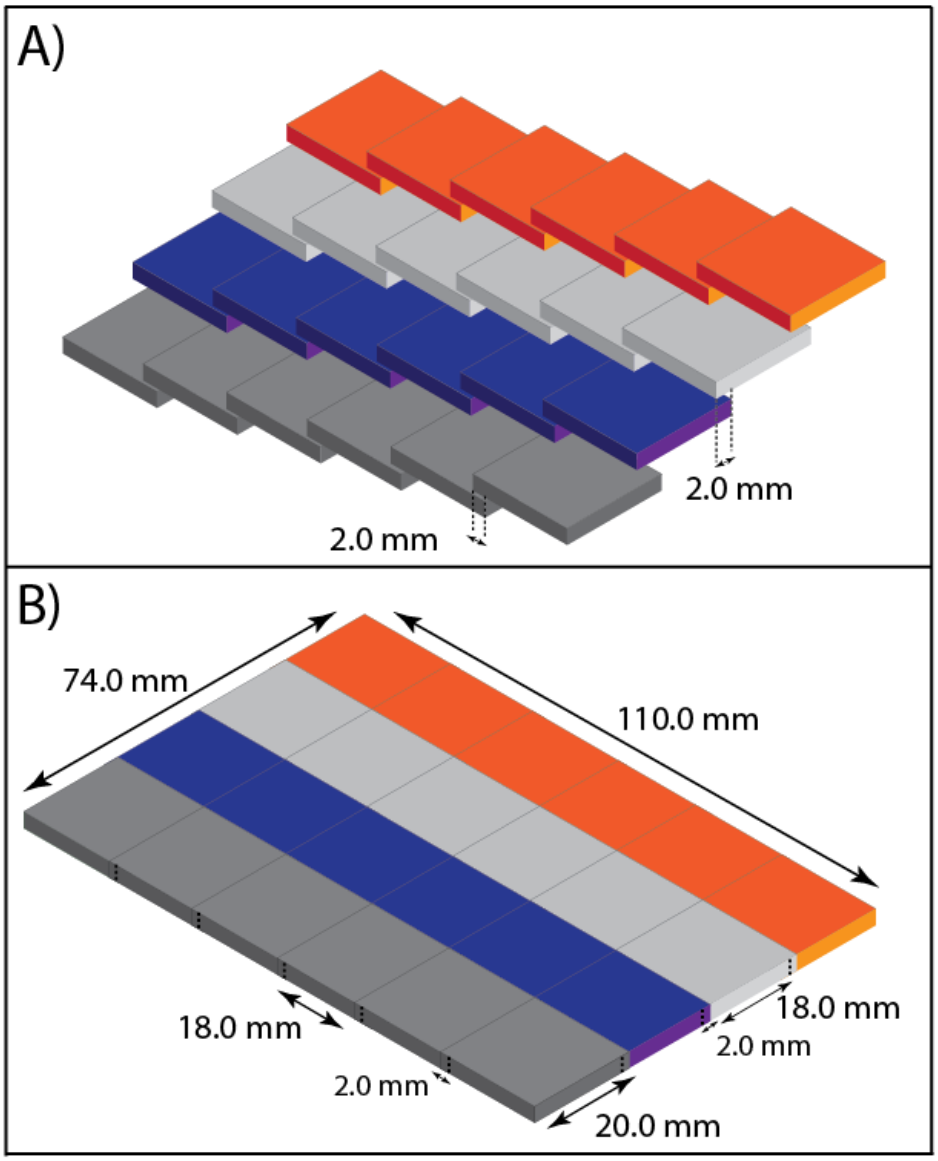

Fig. 4. A) The schematic shows a stack of six times four 20.0 X 20.0 x 8.8 mm^3 OCT images with 2.0 mm overlaps between neighboring scans. Note that the usable depth of OCT imaging is limited to 2-3 mm. B) The schematic illustrates the resulting combined OCT image made from the 24 small images.

In house software (a script in Worldmatch [44]) was used to stitch multiple OCT scans into a single 3D image. Here the probe tilt angle was corrected. Figure 5 shows an example of

Biomedical Optics EXPRESS

the resulting single 3D image.

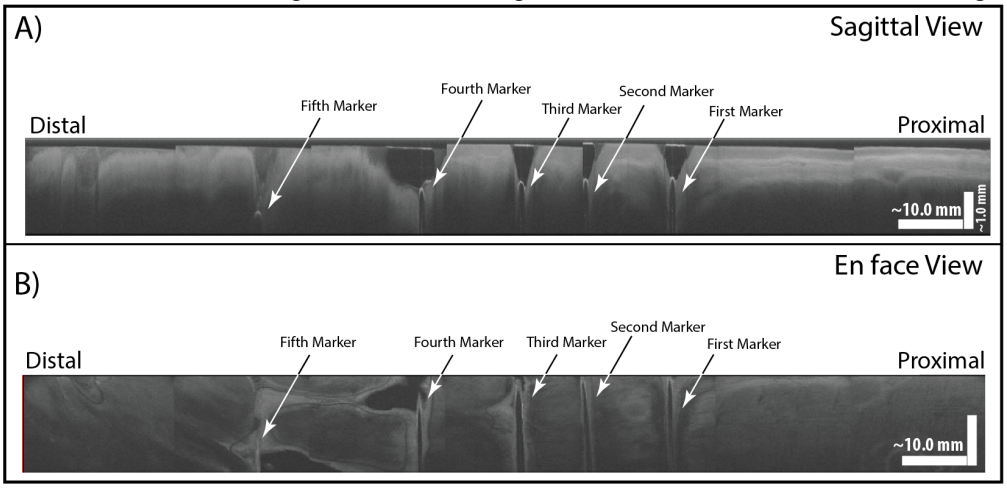

Fig. 5. A) The combined OCT image covers the whole ROI in sagittal view. B) En face view of figure A. Although there are some artifacts at the interface between the OCT images in sagittal view, the resulting image quality is good. Fiducial markers are indicated by arrows.

2.4.1 OCT imaging protocol

We adjusted the marker laser beam of the hand-held OCT probe — using the multimodal moving stage — with respect to the esophageal specimen, guided by the location of the grid lines on top of the glass plate. We validated our distance measurements when the specimen was placed in the correct imaging position by re-measuring the distances between the needle fiducial markers. The water-filled balloon was placed on top of either the specimen (for the specimens that were not pinned on a styrene foam board) or the styrene foam board to diminish the air gaps between the tissues and the gridded glass surface (Fig. 3). We acquired the OCT images by starting at the proximal part of the specimen and moving the stage laterally and then axially, respectively — considering the prescribed 2.0 mm overlap between the scans.

2.5 OCT image processing

We visually inspected the 3D OCT images to identify the borders between the healthy tissue and radiation-induced fibrotic tissue as well as the borders between healthy and/or radiation-induced fibrotic tissue and residual cancer based on the presence or distortion of esophageal layers. Since patients in this study underwent nCRT treatment prior to esophagectomy, we had no untreated tumor visible in the specimen. Therefore, we can only detect residual cancer. We used an in-house developed module for the open source ImageJ software to plot the attenuation of the light at several locations to check if we are able to differentiate esophageal wall layers. The first 3.0 mm of a healthy human esophagus wall consists of epithelium, lamina propria, muscularis mucosa, submucosa, and muscularis propria layer.

2.6 Specimen preparation for histology

The esophageal surgical resection specimen was processed according to routine protocol. It was opened longitudinally and pinned down for optimal fixation in buffered formalin overnight. The complete circumference of the esophagus in the tumor area would be embedded for histological evaluation. The cutting levels were guided by the position of the reference fiducial marker and the ROI for OCT imaging as recorded in the digital photos. A pathologist would cut the specimen into 10 to 14 stripes, parallel to the long axis of the

Biomedical Optics EXPRESS

esophagus — covering the ROI — and (one or more) 4.0 μm histology slides were sectioned from each stripe and stained using haematoxylin and eosin (H&E) according to the standard protocol.

2.7 Histological imaging

For the histopathology analysis, we used a Zeiss Axioskop2 Plus microscope (Carl Zeiss Microscopy, Oberkochen, Germany). Digital microscopic photos of slides were taken with a Zeiss AxioCam HRc digital camera and processed with AxioVision 4 software (both Carl Zeiss Vision, Munich, Germany). Measurements on the microscopic slides were transcribed on macroscopic photos with a ruler placed next to the fresh esophageal excision specimen, enabling OCT to histopathology correlation.

2.8 OCT-histopathology co-localization

Tissue landmarks, such as ridges in the esophageal wall, were used for lateral co-localization. Both histopathology and OCT findings in proximal and distal esophagus were reported based on their longitudinal distances to the reference fiducial marker. Since the OCT analysis was based on fresh specimens while histopathology was done after formalin fixation procedure, we measured and corrected for tissue shrinkage.

We measured the distance between adjacent fiducial markers several times at various stages in the procedure as well as the distance between the most proximal and distal fiducial markers. We first measured these distances (Fig. 2) after inserting the needle fiducial markers and repeated our measurements when the tissue was placed on the OCT scanning apparatus. After ink marking, we re-measured the distances to make note of possible deviations compared to the recorded distances based on the needles. We measured the distances for the last time post formalin fixation procedure to estimate the total shrinkage/expansion factor. We decided to solely consider the distance between the most proximal and the most distal fiducial markers for shrinkage/expansion calculation.

We defined shrinkage rate S_1 as the distance ratio between needle fiducial markers and ink markings as follows:

$$S_1 = \frac{D_{inked}}{D_{needle}}. \tag{1}$$

where D_{needle} is the distance between needle fiducial markers (in our case: between the first and the last needle fiducial markers) and D_{inked} is the distance between corresponding ink fiducial markers before fixation. Similarly, we calculated the shrinkage rate between the fresh tissue and the formalin-fixated tissue (S_2) as follows:

$$S_2 = \frac{D_{fixated}}{D_{inked}}. \tag{2}$$

where $D_{fixated}$ is the distance between ink fiducial markers after fixation (in our case: between the first and the last fiducial markers). Although we expect S_2 always to be <1 (shrinkage), in practice, values >1 were found for the first 5 patients because they were imaged prior to the pinning step which stretched the tissue. We considered fresh specimens as our reference; therefore, we reported histopathology findings on the OCT scale. We transformed measured distances of histopathology analysis to the fresh esophageal specimen as follows:

$$M_{pathology} = M_{OCT} \cdot S_1 \cdot S_2. \tag{3}$$

Biomedical Optics EXPRESS

where $M_{pathology}$ is a shrinkage or expansion corrected measurement in histopathology and M_{OCT} is a measured distance in OCT images. Because of missing data we could not estimate the shrinkage for the first three patients. We therefore used the average shrinkage of patients four and five instead (acquired with the same protocol).

2.9. PTV and GTV correlation with radiation-induced fibrosis and residual cancer regions

We investigated the correlation between the PTV and the GTV from planning CT images with the regions of radiation-induced fibrosis and residual cancer in histopathology analysis. We measured the length of PTV and GTV in CT images using Oncentra treatment planning software (Elekta, Stockholm, Sweden), approximating the curved esophagus with several straight lines (Fig. 6). Because of unknown shrinkage between the in vivo situation and the fresh specimen, lengths were measured relative, i.e., as a percentage of the esophageal length — starting 21 cm below the teeth level (a standard used depth of the intrathoracic anastomosis) to the stomach. We determined similar length ratio of the detected radiation-induced fibrosis regions and the residual cancer regions based on the histopathology reports and resected specimen photos (Table 2 and 3). We measured PTV and radiation-induced fibrosis lengths in patients that showed fibrosis in both histopathology and OCT analysis (Table 1). Similarly, we measured GTV and residual cancer lengths in patients that showed residual cancer in both histopathology and OCT analysis. To assess overall shrinkage after esophagectomy, we determined the overall shrinkage difference between resected esophageal specimens and intact esophagi for patients that were included in either of the above measurements (patients 1, 4, 5, 6, 7, 8, and 10).

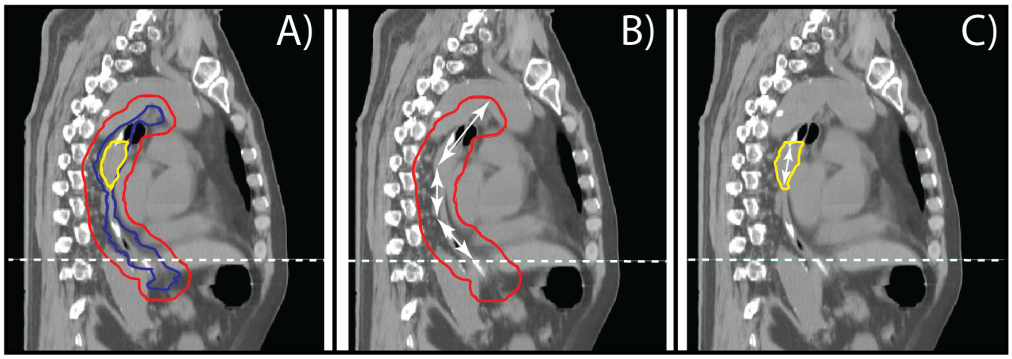

Fig. 6. A) This CT image shows GTV (yellow), CTV (blue), and PTV (red) in a sagittal view. The dashed line represents the stomach level. B) Illustration of PTV length measurement. C) Illustration of GTV length measurement.

3. Results and discussions

The average longitudinal shrinkage for the last five patients was 6.5% or 1.5 mm with a standard deviation of 1.1 mm (range: 0.14-2.56 mm, median 1.9 mm). Guided by histopathology, we detected radiation-induced fibrosis in the OCT images as the distortion and/or loss of part of the esophageal wall layering structure (Fig. 7). The absence of layers corresponded with residual or treated cancer (Fig. 7(C)). The absence of residual cancer indication in histopathology may indicate a pCR. Figure 8 represents corresponding OCT and histopathology images indicating healthy, fibrotic, and residual cancer areas. The OCT and histopathology results are summarized in Table 1. The overall sensitivity and specificity of OCT to detect radiation-induced damage and residual cancer matched with histopathology, were 79% and 67% respectively.

Biomedical Optics EXPRESS

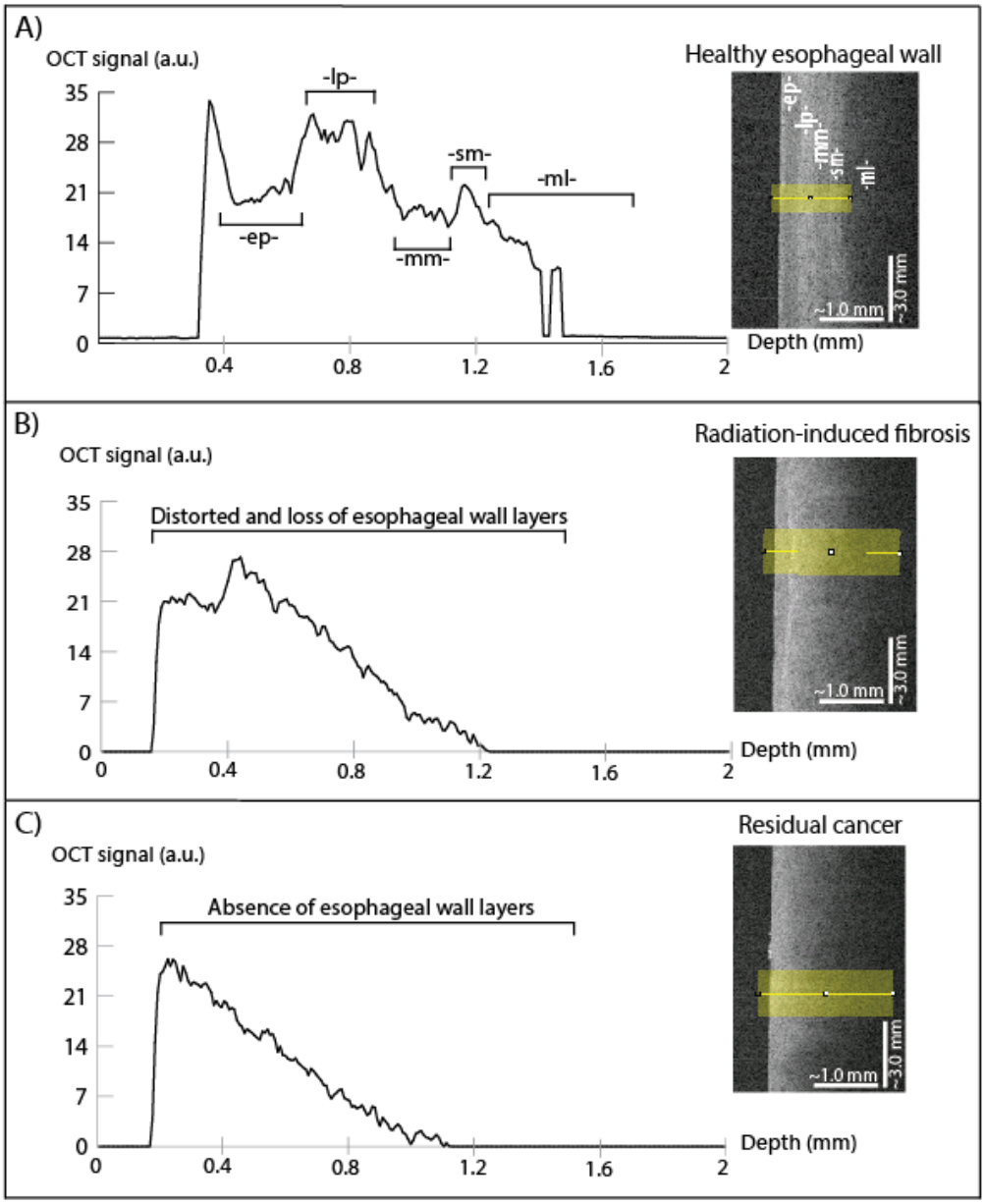

Fig. 7. A) OCT image and plot showing esophageal wall layers of a healthy part of the esophagus (epithelium (ep), lamina propria (ep), muscularis mucosa (mm), submucosa (sm), and muscle layers (ml)). B) OCT image and plot illustrating radiation-induced fibrosis with partial loss of esophageal wall layers. C) OCT image and plot illustrating residual cancer. . Note that tails of the OCT signals (beyond 1.2-1.5 mm) in A and B were very noisy have been set to 0 for visual representation.

Biomedical Optics EXPRESS

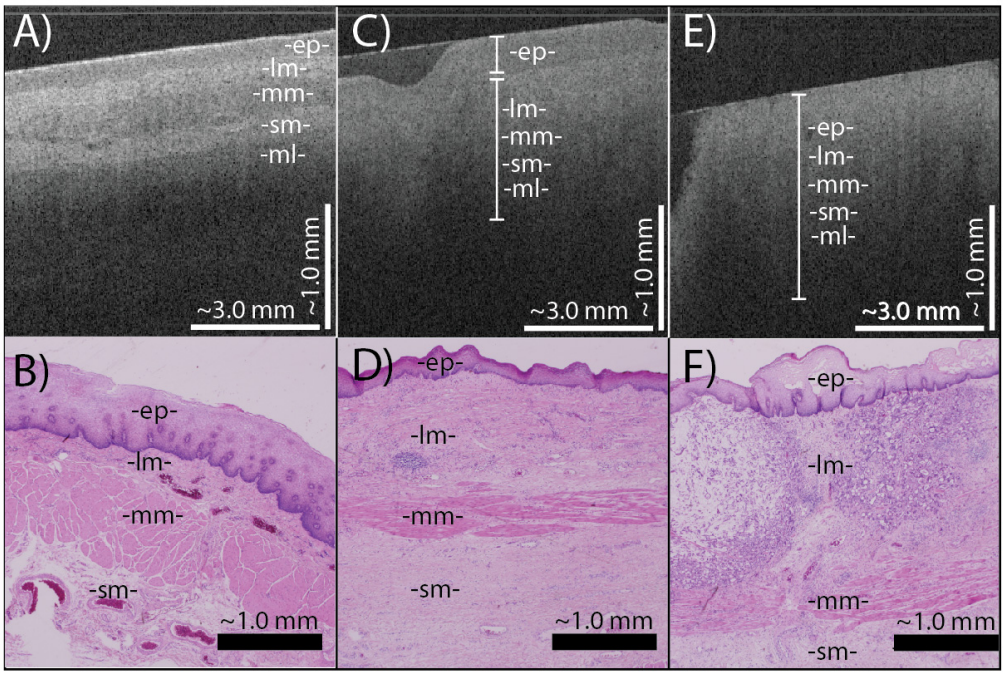

Fig. 8. A) and B) show the corresponding esophageal wall layers of a healthy part of the esophagus (epithelium (ep), lamina propria (ep), muscularis mucosa (mm), submucosa (sm), and muscle layers (ml)) on OCT and histopathology, respectively (patient 7). C) and D) represent the corresponding radiation-induced fibrosis on OCT and histopathology (patient 7). E) and F) show the corresponding residual cancer on OCT and histopathology (patient 10).

Table 1. Overview of patients, their tumor regression grading (TRG) score, histopathology and OCT analysis to identify the border between 1) healthy tissue and radiation-induced fibrosis, and between 2) healthy tissue and/or fibrosis and residual cancer. "Positive" means that we identified the border in OCT or histopathology. TRG 1: fibrosis without detectable residual tumor cells; TRG 2: fibrosis with rare residual tumor cells; TRG 3: fibrosis and residual tumor cells with preponderance of fibrosis; TRG 4: fibrosis and residual tumor cells with preponderance of tumor cells, TRG 5: no tumor regression.

Patient	Gender	Age	TRG Score	Healthy tissue / fibrosis border presence		Residual cancer presence	
				Histopathology	OCT	Histopathology	OCT
1	Male	70	4	Negative	Positive	Positive	Positive
2	Female	50	3	Positive	Negative	Negative	Positive
3	Male	57	2	Negative	Negative	Negative	Negative
4	Female	60	1	Positive	Positive	Negative	Negative
5	Male	63	2	Positive	Positive	Positive	Positive
6	Male	75	3	Positive	Positive	Positive	Positive
7	Male	67	2-3	Positive	Positive	Positive	Positive
8	Female	70	2	Positive	Positive	Positive	Positive
9	Male	50	4	Negative	Negative	Positive	Negative
10	Male	70	4	Positive	Negative	Positive	Positive

3.1 Radiation-induced fibrosis

We summarized the histopathology and OCT findings regarding the border between radiation-induced fibrosis and healthy tissue in Table 2. For proximal and distal sections, we reported the distance to the reference fiducial marker at three lateral levels (right, left, and

Biomedical Optics EXPRESS

center) used for the histopathology report (Fig. 9). The relative lateral levels of OCT and histopathology were defined for each patient and therefore are not comparable between patients. The sensitivity and specificity of OCT to detect radiation-induced damage were 71% and 67%, respectively (Table 1). We calculated sensitivity and specificity based on visual scoring.

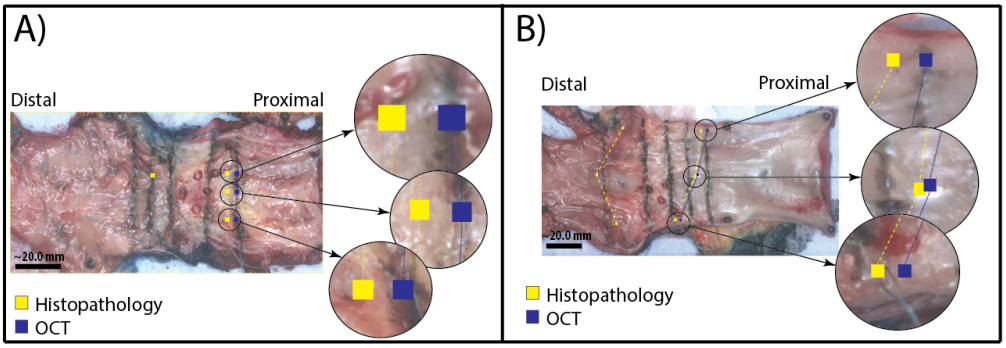

Fig. 9. A) and B) show the correlation of histopathology and OCT defined borders between radiation-induced fibrosis and healthy tissue for two patients (patient 6 and 7, respectively) in the proximal and distal esophagus.

Figure 10 shows the difference between OCT and histopathology in finding the proximal and distal radiation-induced fibrotic and healthy tissue border for all the corresponding findings in OCT images and histopathology results (n = 14). The overall absolute difference of distances from the border to the reference fiducial marker between OCT and histopathology on average was 5.0 ± 4.6 mm (range: 0.4-17.4 mm, median 3.6 mm).

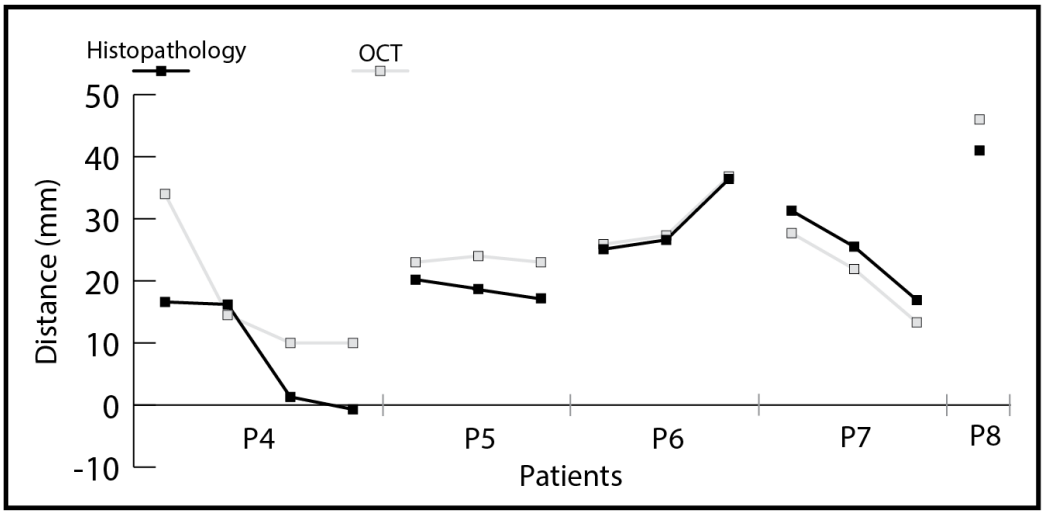

Fig. 10. Distance between reference marker and radiation-induced fibrosis and healthy tissue border in OCT and histopathology.

Biomedical Optics EXPRESS

Table 2. Overview of the histopathology and OCT analysis of the border between radiation-induced fibrosis and healthy tissue in three lateral levels in the proximal and distal esophagus. The numbers represent the distances between these borders and the reference fiducial markers for each specimen at the different lateral levels used for pathology. Patients that showed fibrosis with no healthy tissue in both histopathology and OCT were excluded from this table. "–" indicates that we could not identify the borders. Patients that did not show any radiation-induced fibrosis in histopathology were excluded from this table. Only patients that showed at least one correspondent measurements for both histopathology and OCT were presented.

Distance to reference marker (mm)							
		Histopathology		OCT		Difference (OCT and Histopathology)	
Patient	Level	Proximal	Distal	Proximal	Distal	Proximal	Distal
4	L1	16.6	0.3	34.0	–	17.4	–
	L2	16.2	1.3	14.5	10.0	–1.7	8.7
	L3	3.3	–0.7	–	10.0	–	10.7
5	L1	20.2	19.2	23.0	–	2.8	–
	L2	18.7	17.7	24.0	–	5.3	–
	L3	17.2	17.7	23.0	–	5.8	–
6	L1	25.1	8.7	25.9	–	0.8	–
	L2	26.6	–	27.3	–	0.7	–
	L3	36.4	–	36.8	–	0.4	–
7	L1	31.3	34.9	27.7	–	–3.6	–
	L2	25.5	38.9	21.9	–	–3.6	–
	L3	16.9	21.9	13.3	–	–3.6	–
8	L1	31.7	31.7	–	–	–	–
	L2	34.2	36.2	–	–	–	–
	L3	41.0	31.2	46.0	–	5.0	–

3.2 Residual cancer

It was more complicated to identify the residual cancer since the surrounding region consisted mostly of radiation-induced fibrosis, which already had a distorted and/or incomplete esophageal wall-layering structure. However, guided by histopathology, we found that the esophageal wall layering is absent in residual cancer areas (Fig. 7(C)). Our OCT and histopathology findings in terms of proximal and distal distance from the border (healthy tissue and/or fibrosis and residual cancer) to the reference fiducial marker are provided in Table 3. Histopathology reports were more detailed for the reported distances to the reference fiducial marker — than those from the radiation-induced fibrosis. Hence, we could report on more lateral levels (compared to three lateral levels reported for radiation-induced fibrosis). We demonstrated residual cancer delineation in the OCT images and histopathology in Fig. 11. Figure 12 shows OCT and histopathology distance measurements between the reference marker and identified borders between residual cancer and healthy or fibrotic tissues in proximal and distal esophageal regions (n = 68).

Biomedical Optics EXPRESS

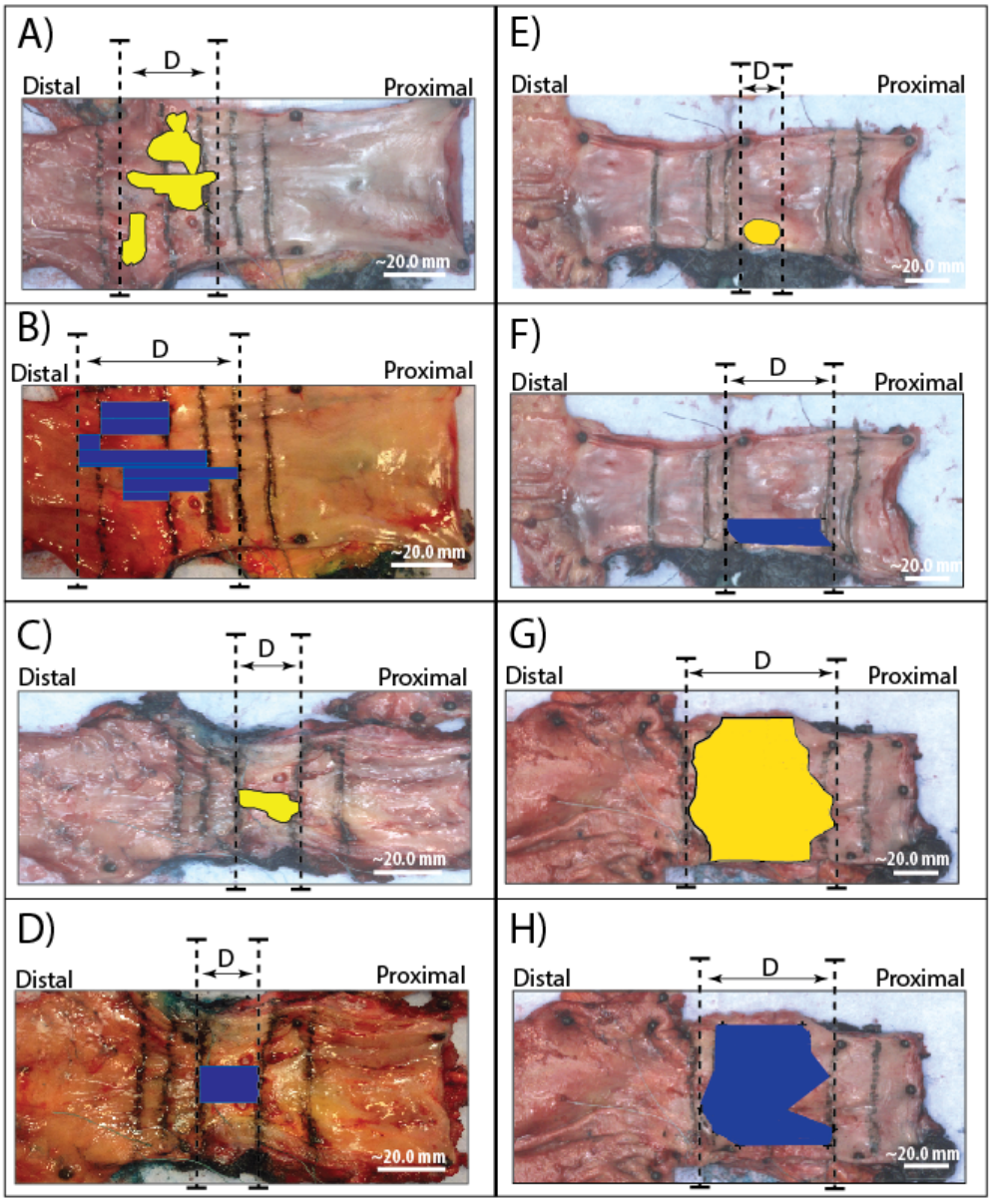

Fig. 11. A) and B) show the location of residual cancer in a patient's esophagus (patient 7) in histopathology (in yellow) and OCT (in blue), respectively. The maximum longitudinal lengths of the residual cancer regions healthy are shown by "D". Similarly, C) and D), E) and F), and G) and H) demonstrate the residual cancer regions of patients 6, 8, and 10 in histopathology (in yellow) and OCT (in blue).

Biomedical Optics EXPRESS

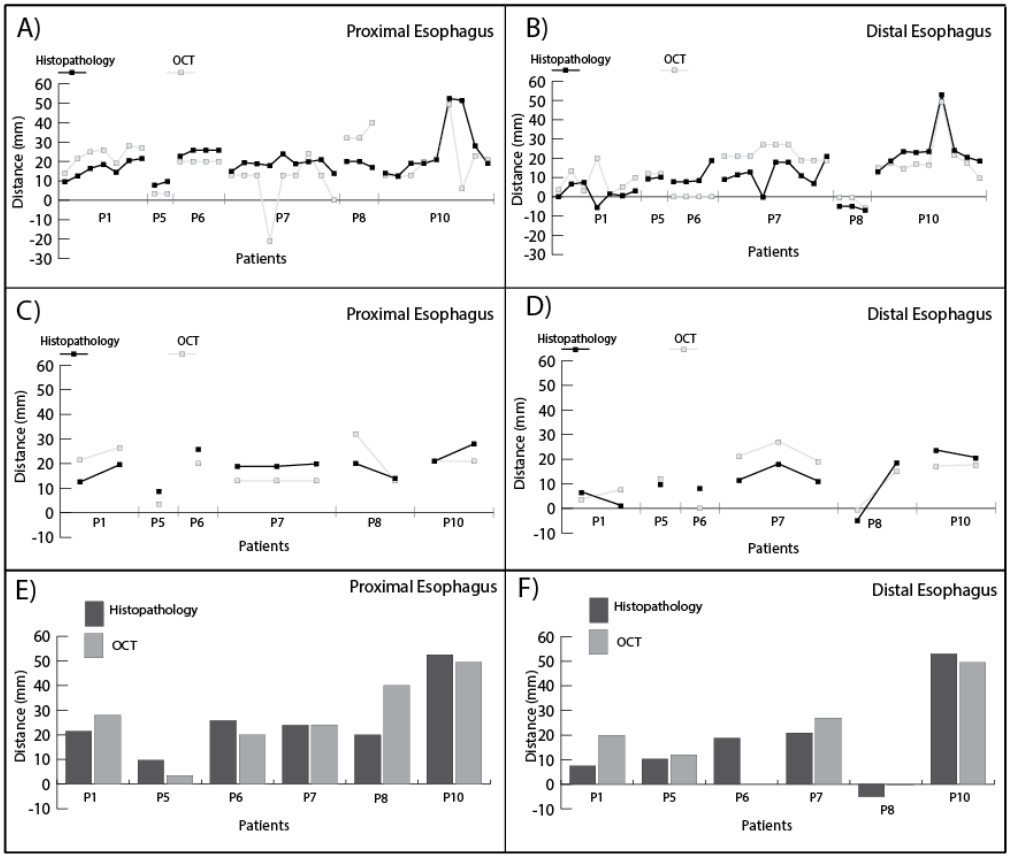

Fig. 12. A, B) Distance measurements in OCT and histopathology. The graphs demonstrate the distance between residual cancer and healthy tissue/radiation-induced fibrosis border to the reference fiducial marker in proximal and distal esophagus. C, D) Also show these distances while reducing the data points using the medians between neighboring measurements to eliminate outliers. E, F) The graphs show the maximum distance from the reference fiducial markers to the identified borders in proximal and distal esophagus.

The sensitivity and specificity of OCT to detect residual cancer matched with histopathology, were 86% and 67%, respectively (Table 1). However, in patient 9, the residual cancer was located at a depth of ~10.0mm in the esophageal wall, which is outside of the visibility range of OCT. The overall absolute difference of distances from the border to the reference fiducial marker between OCT and histopathology on average was 7.9 ± 8.1 mm (range: 0.0-45.5 mm, median 6.0 mm).

Biomedical Optics EXPRESS

Table 3. Overview of the histopathology and OCT analysis of identification of residual cancer borders in several lateral levels in proximal and distal esophagus. The numbers represent the distances between the borders and the reference fiducial markers for each specimen. Patients that did not show any residual cancer in either histopathology or OCT were excluded from this table.

		Distance to reference marker (mm)					
		Histopathology		OCT		Difference (OCT and Histopathology)	
Patient	Level	Proximal	Distal	Proximal	Distal	Proximal	Distal
1	L1	9.5	0.0	14.0	3.5	4.5	3.5
	L2	12.5	6.5	21.5	13.5	9.0	7.0
	L3	16.5	7.5	25.0	3.0	8.5	–4.5
	L4	18.5	–5.5	26.0	20.0	7.5	25.5
	L5	14.5	1.5	19.0	1.5	4.5	0.0
	L6	20.5	0.5	28.0	5.0	7.5	4.5
	L7	21.5	3.0	27.0	10.0	5.5	7.0
5	L1	7.7	9.2	3.5	12.0	–4.2	2.8
	L2	9.7	10.2	3.5	12.0	–6.2	1.8
6	L1	22.8	7.8	20.0	0.0	–2.8	–7.8
	L2	25.8	7.8	20.0	0.0	–5.8	–7.8
	L3	25.8	8.3	20.0	0.0	–5.8	–8.3
	L4	25.8	18.8	20.0	0.0	–5.8	–18.8
7	L1	14.9	8.9	13.0	21.0	–1.9	12.1
	L2	19.4	11.4	13.0	21.0	–6.4	9.6
	L3	18.9	12.9	13.0	21.0	–5.9	8.1
	L4	17.9	–0.1	–21.0	27.0	–38.9	27.1
	L5	23.9	17.9	13.0	27.0	–10.9	9.1
	L6	18.9	17.9	13.0	27.0	–5.9	9.1
	L7	19.9	10.9	24.0	19.0	4.1	8.1
	L8	20.9	6.9	13.0	19.0	–7.9	12.2
	L9	13.9	20.9	0.0	19.0	–13.9	–1.9
8	L1	20.0	–5.0	32.0	–0.5	12.0	4.5
	L2	20.0	–5.0	32.0	–0.5	12.0	4.5
	L3	17.0	–7.0	40.0	–6.0	23.0	1.0
10	L1	14.0	13.0	13.0	15.0	–1.0	2.0
	L2	12.5	18.5	12.0	17.5	–0.5	–1.0
	L3	19.0	23.5	13.0	14.5	–6.0	–9.0
	L4	19.0	23.0	20.0	17.0	1.0	–6.0
	L5	21.0	23.5	21.0	16.5	0.0	–7.0
	L6	52.5	53.0	49.5	49.5	–3.0	–3.5
	L7	51.5	24.0	6.0	21.5	–45.5	–2.5
	L8	28.0	20.5	23.0	17.5	–5.0	–3.0
	L9	19.0	18.5	21.0	9.5	2.0	–9.0

3.3 PTV and GTV correlation with radiation-induced fibrosis and residual cancer

On average, the esophageal specimens had 42% shrinkage compared with the intact esophagus. Our relative length measurements verified the rough correspondence of length ratios between PTV and radiation-induced fibrosis after RT (Fig. 13). The overall absolute value of length-ratio differences between PTV and radiation-induced fibrosis was 14%. The overall absolute value of length-ratio differences between GTV and residual cancer was 9%.

Biomedical Optics EXPRESS

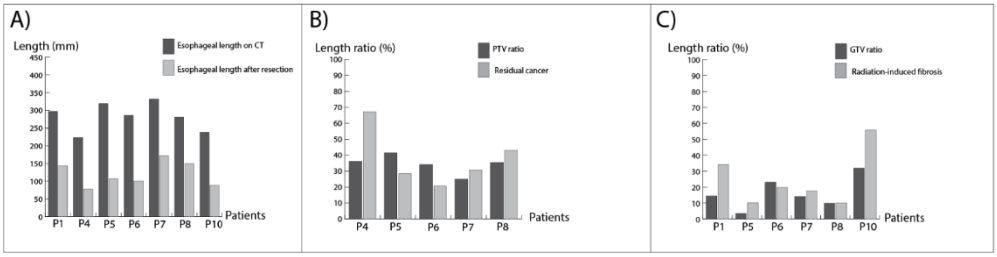

Fig. 13. A) Length of the esophagus on CT and after esophagectomy. B) The absolute value of the length ratios of the PTV and radiation-induced fibrosis regions. C) The graph shows the absolute value of the length ratios of the GTV and residual cancer regions.

3.4 Discussion

In this study, we investigated the feasibility of OCT for ex vivo identification of radiation-induced fibrosis and residual cancer (as detected on histopathology) in 10 esophageal cancer patients treated with nCRT followed by esophagectomy. We found radiation induced effects as distortion of the mucosal layers at OCT and residual tumor as absence of layers. We matched our findings and guided our identification with histopathology as the gold standard. Moreover, we determined and compared the most proximally and distally located borders between healthy tissue, radiation-induced fibrosis, and residual cancer at various axial levels on OCT and histopathology. Our results showed that OCT can detect radiation-induced fibrosis and residual cancer with the sensitivity of 71% and 67% and specificity of 86% and 67%, respectively. Overall, the absolute difference between OCT and histopathology on average was 5.0 ± 4.6 mm for the borders between healthy tissue and radiation-induced fibrotic tissue and 7.9 ± 8.1 mm for the borders between healthy/fibrotic tissue and residual cancer. We also verified the correlation of PTV and GTV length estimates performed on the RT planning CT scan with the length of radiation-induced fibrosis and residual cancer regions assessed at histopathology. Our data shows that OCT has potential to help in response assessment in order to select patient for organ preservation after nCRT. However, our results were ex vivo and tests using in vivo OCT and double blind evaluation are necessary. Inflatable OCT probes and dedicated OCT imaging systems for in vivo OCT imaging of the esophageal wall in 3D are available [28,37,45].

When identifying radiation-induced fibrosis using OCT, we could mainly locate the proximal border. The reason was that most of the primary tumors were located distally in our cases. The fibrotic tissue extended often very close to the level of stomach, which hampered distal morphological differentiation between healthy regions and fibrosis on OCT. However, histopathology could detect the distal border. Although we found a difference between the appearance of fibrosis and residual cancer on OCT, it was easier to differentiate between healthy tissue and radiation-induced fibrosis than between radiation-induced fibrosis and residual cancer because of the more distinct esophageal wall layering of the healthy tissue regions. Hence, identifying residual cancer is complicated. We defined residual cancer as the absence of esophageal layering and compared our OCT findings with histopathology. We concluded that nonappearance of residual cancer may suggest pCR. It is possible that in case of a pCR the OCT images may still contain regions without esophageal wall layering since it is unknown if the mucosal layers displaced by the tumor will all restore after nCRT. This was however not the case in our data compared with pathology. In addition, in this study we analyzed OCT images only at pathology locations. The results of this study are presented in two complementary ways; as sensitivity and specificity based on visual scoring and as distance measurements between the reference fiducial markers and radiation-induced fibrosis and healthy tissue borders as well as between the reference fiducial markers and residual cancer and healthy/radiation-induced fibrosis borders on OCT and histopathology. A validation of the change of OCT signal over depth associated with the visually identified

Biomedical Optics EXPRESS

regions on an independent data set is considered outside of the scope of the current feasibility study. We identified the longitudinal boundaries between radiation-induced fibrosis and healthy tissue as well as between healthy tissue and/or fibrosis and residual cancer on the same slide in histopathology analysis. However, the boundaries could be presented either on the same or on adjacent longitudinal slides. The identification between healthy tissue, radiation-induced fibrosis, and residual cancer was solely based on visual scoring in both histopathology and OCT by experts. Our visual analysis of the OCT signal utilized the depth profile. Histopathology was used as ground truth, i.e., in case histopathology showed no tumor but OCT did, it was scored as a false-positive (Table 1). However, due to under-sampling in the histopathology residual cancer regions may have been missed; Hence the ground truth has its limitations. Further validation included comparison of distances between the borders of tissue types (relative to the reference fiducial markers) between OCT and histopathology. In future work, automated OCT analysis may help to detect pCR with a high resolution, as we would not be limited to a few pathology slides. However, the limitation of usable OCT imaging depth of up 2.0 to 3.0 mm hampers its ultimate sensitivity.

Our fiducial markers were visible on OCT, thus, our proposed method to calculate the longitudinal shrinkage was effective. The overall reduction in length of the esophagus in situ to the fixed specimen is expected to be 50%, while the tumor changes little in length [46]. Our measurements agree with this. The histopathology method of pinning the specimen to a styrene foam board kept shrinkage after surgery at a minimal level. Reference fiducial markers obscured small part of the OCT images, which may hamper the precise boundary identification (Fig. 5).

The challenge of RT is to accurately deliver the radiation dose to the tumor and tumor-involved lymph nodes while sparing the surrounding healthy tissues. Tumor extent delineation is a crucial step in the RT planning process. Endoscopy or endoscopic ultrasound (EUS) is used to assess the macroscopic tumor extension, which help tumor delineation on CT. EUS is hampered by under- and over-staging due to the microscopic tumor extensions smaller than the EUS resolution and because of the inability to differentiate between inflammatory changes and tumor infiltration [47–50]. Therefore, safety margins of ~3 cm are typically used in the craniocaudal tumor directions around the GTV. The OCT has higher resolution than the EUS. Future research, including in vivo OCT imaging, may demonstrate the feasibility of OCT to accurately determine tumor extent and inflammatory changes for RT planning and thereby allow for more accurately defined radiation fields with smaller safety margins. Moreover, more patients could be considered, validation in an independent cohort should be performed, and inter-observer agreement of OCT and histopathology findings should be determined. While registering information from both EUS and OCT to the planning CT is challenging, fiducial markers may facilitate the OCT and planning CT registration [28]. To prove the potential of OCT in tumor boundary identification, it would be better if we could scan these patients in vivo prior to nCRT, where the gross tumor is present. However, ex vivo OCT imaging of gross tumor operable patients who did not undergo nCRT may better show the feasibility to detect tumor extent for RT planning. Figure 13 shows that the length of the GTV is smaller than the length of the residual cancer region at histopathology in patients one, five, seven, and 10. This suggests the necessity of adding a safety margin around the GTV to include subclinical disease spread to create the CTV. More clinical in vivo OCT imaging trials are necessary using commercially available OCT devices dedicated to esophageal imaging, which are capable of visualizing esophageal layers from epithelium to the muscle layers [28]. Furthermore, multiple OCT scans at various treatment stages are useful to monitor the tumor reaction to nCRT. Quantitative analysis of the OCT images, i.e., using the attenuation coefficient of the OCT signal over depth could be the next step to validate our results.

Biomedical Optics EXPRESS

4. Conclusions

In conclusion, we studied the feasibility of OCT to detect the proximal and distal borders of radiation-induced fibrosis and residual cancer ex vivo in esophageal specimens from 10 patients who underwent nCRT followed by esophagectomy. Overall sensitivity and specificity of OCT to differentiate between healthy tissue, fibrotic tissue, and residual cancer were 79% and 67%, respectively. Our findings indicated that OCT is capable of detecting radiation-induced fibrosis and residual cancer in the human esophagus.

Funding

Netherlands Organization for Health Research and Development (ZonMw); Elekta; NinePoint Medical, Inc.

Acknowledgments

The authors would like to thank Niek van Wieringen for useful discussion.

Disclosures

Dr. T. Alderliesten is involved in projects supported by Elekta. Prof. H.W.M van Laarhoven is involved in researches supported by Bayer B.V., Bristol-Myers Squibb, Celgene, Janssen & Janssen, Lilly, Nordic Pharma, Philips, and Roche and is consultant to Bristol-Myers Squibb, Lilly, and Nordic Pharma. Prof. M.I. van Berge Henegouwen is involved in projects supported by Olympus and is consultant to Medtronic and Janssen & Janssen. Prof. J.F. de Boer is a beneficiary of patents that are licensed to NinePoint Medical, Inc. Elekta, NinePoint Medical, Bayer B.V., Bristol-Myers Squibb, Celgene, Janssen & Janssen, Lilly, Nordic Pharma, Olympus, Philips, Medtronic, and Roche had no involvement in the study design, the data collection, analysis and interpretation, and the writing of the manuscript.